Stray Light Correction for Imager

KIGAWA Seiichiro*

Abstract

The Multi-functional Transport Satellite (MTSAT)-2 Imager has a channel wavelength of 3.75 micrometers, and it is expected that the channel will be effective in the detection of nighttime fog and low-level clouds. In this wavelength, it is known from the observation data of Geostationary Operational Environmental Satellite (GOES) Imagers that stray light in the imager is observed around midnight. Thus a technique was developed for predicting and correcting the stray light. The stray light is predicted by estimate equations based on physical considerations, and the observed data is corrected by predicted stray light. The verification of the equations was conducted using the GOES Imager data, and it showed that an estimation error of 1 Kelvin or less would be achieved. Furthermore, it seems that the striped pattern observed on GOES Sounders will be reduced by the application of the estimating technique of the stray light. This report describes the summary of the stray light correction that will be operated for MTSAT-2.

1. Introduction

Stray light is defined as the undesired light that is detected as a signal excluding objective light at an optical instrument. The stray light is often generated due to the reflection and/or scattering on the inside walls and optical components of the optical instrument.

The stray light generated in the Imager is caused by the scattering of sunlight inside the Imager around midnight, which appears as a ghost on cloud imagery. Since the stray light is prominent in shorter wavelength, the Visible and IR4 (3.75 micrometers, called shortwave infrared) bands of MTSAT-2 are affected strongly. Because the stray light is added into the radiance of the cloud imagery, the imagery is brighter in the visible channel, and temperature shifts to higher temperature regions in the shortwave infrared due to the stray light. Most of the visible imagery shows nighttime regions around midnight, that is, the period when the stray light appears, so that substantially there is no influence of the stray light in the visible channel. However it is required to remove the stray light to keep the effectiveness of the shortwave infrared, because it is especially effective to detect fog and low-level clouds at night.

This report describes the summary of the stray light correction that will be operated for MTSAT-2.

2. Relation between Stray Light and Wavelength

First, let us think why the sun is the principal source for the stray light. Figure 1 shows a comparison between the solar and earth

radiance calculated by the Planck function. In the left figure, the horizontal axis indicates wavelength and the vertical one indicates radiance. The curve plotted toward the upper right of the figure shows radiance from the blackbody of a temperature of 300 K, and another curve plotted toward lower right shows the solar radiance when the reflectance of the earth is 1. A boundary at 4.6 micrometers is observed to divide the thermal infrared and near (shortwave) infrared sides. The radiance from the 300 Kelvin blackbody is greater on the thermal infrared side, while the solar radiance is prominent on the shortwave infrared side. The right figure shows the ratio of the solar radiance to the radiance of the 300 Kelvin blackbody in the vertical axis. It shows that the ratio at the shortwave infrared is over 100 times greater than a 6.75 micrometers (water vapor) channel. From these figures, it can be thought that the stray light is prominent at the shortwave infrared.

Now thinking that incident light is perpendicular to a surface that has random gaps in the vertical axis, as shown in Figure 2, although this surface is different from a Lamellar grating, due to a random surface pattern, it can be understood intuitively that diffraction light is generated at this surface. The incident light that is perpendicular to the surface returns to the direction of the light source. When the surface reflects the light, a wave front error is generated, and the intensity ratio of reflected light to the incident light is expressed as (M. Born and E. Wolf: 1975)

$$1 - \left(\frac{4 \cdot \pi \cdot \sigma}{\lambda} \right)^2 \tag{1}$$

where σ is the standard deviation of surface roughness, and λ is the wavelength of the light. The second term means diffraction light and it may be interpreted as scattered light. Therefore, it is shown from Equation (1) that the scattered light is proportional to the square of the surface roughness and inversely proportional to the square of the wavelength. Although the real surface has complicated patterns, so that multi-scattering should also be considered, it is expected that Equation (1) can be used as a first-order approximation.

A candidate for the source of the stray light on the Imager is a light source outside the Imager. Since it is thought that light from the satellite structure is removed at the Imager's optical port (sun shield), the sun, moon, or earth could be the light source. Figure 3 shows the radiance ratio of the 300 Kelvin blackbody to the stray light on condition that the surface roughness of the mirror, σ, is 10 nm, and the scattered light is distributed uniformly in all directions. This ratio means a signal to noise ratio if the stray light is considered as noise. These ratios are given by

$$(\text{SUN}): \quad \frac{B_{300K,\lambda}}{B_{6000K,\lambda}} \cdot \frac{1}{\frac{\Omega_{sun}}{2\pi} \cdot \left(\frac{4\pi\sigma}{\lambda} \right)^2} \tag{2}$$

$$(\text{EARTH}): \quad \frac{B_{300K,\lambda}}{B_{282K,\lambda} + B_{6000K,\lambda} \cdot \frac{\Omega_{sun}}{2\pi} \cdot A_{earth}} \cdot \frac{1}{\frac{\Omega_{earth}}{2\pi} \cdot \left(\frac{4\pi\sigma}{\lambda} \right)^2} \tag{3}$$

$$(\text{MOON}): \quad \frac{B_{300K,\lambda}}{B_{400K,\lambda} + B_{6000K,\lambda} \cdot \frac{\Omega_{sun}}{2\pi} \cdot A_{moon}} \cdot \frac{1}{\frac{\Omega_{moon}}{2\pi} \cdot \left(\frac{4\pi\sigma}{\lambda} \right)^2} \tag{4}$$

where B is the Plank function (radiance in temperature, T, and wavelength, λ). Ωsun, Ωearth, and Ωmoon are the solar, lunar, and earth solid angles respectively. Aearth and Amoon are the albedo of the earth and moon respectively.

Because the radiance that is observed by the Imager is quantized by a 10-bit word, assuming that the stray light is prominent when the signal to noise ratio shown in Figure 3 is less than 1000, it is predicted that the source of the stray light is the sun and the effect of the stray light is limited to the shortwave infrared.
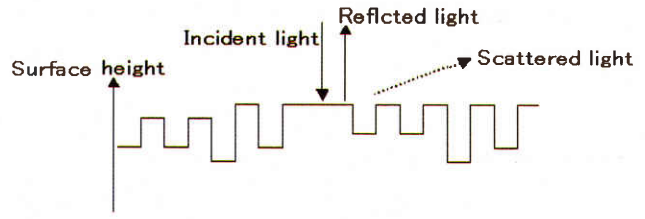

Figure 2. Simplified Surface Shape

If the surface that reflects light is considered as a composition of Lamellar grating, the principles of stray light generation can be understood.
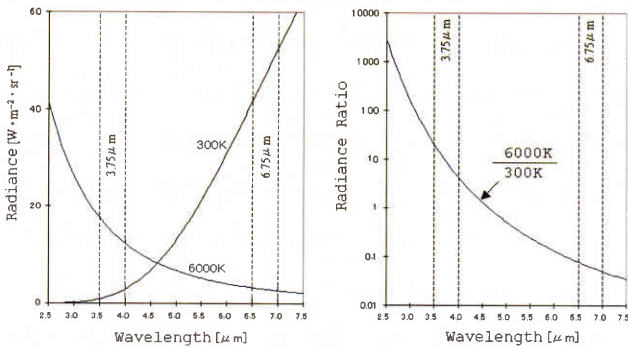

Figure 1. Comparison between Solar and Earth Radiance

Left figure: showing wavelength in the horizontal axis and radiance in the vertical axis, the curve drawn to the upper right of the figure shows radiance from the blackbody of a temperature of 300 Kelvin, and another curve plotted to the lower right shows the solar reflected radiance.

Right figure: the radiance ratio of the solar reflected to the 300 Kelvin blackbody is shown in the vertical axis. It shows that the ratio at the shortwave infrared is over 100 times greater than a 6.75 micrometers (water vapor) channel.
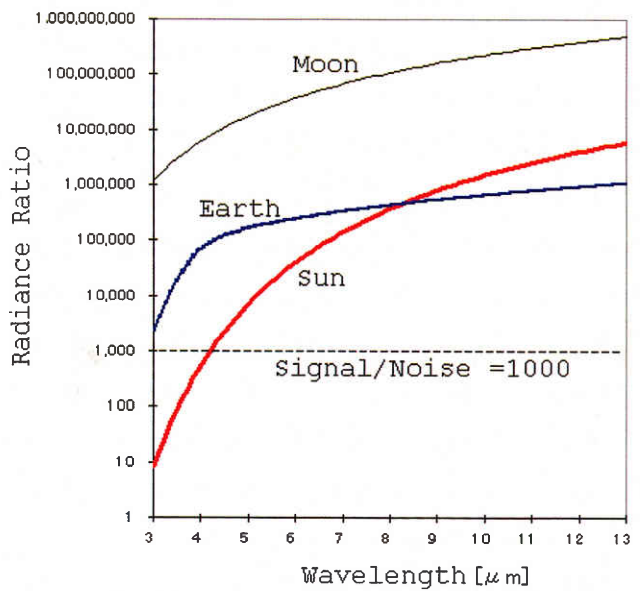

Figure 3. Radiance Ratio of 300-Kelvin Blackbody to Stray Light

This is plotted showing wavelength in the horizontal axis and the radiance ratio of the 300 Kelvin blackbody to the stray light in the vertical axis. If the stray light is considered as noise, this figure shows a signal to noise ratio. The stray light is calculated on condition that the surface roughness of a mirror, σ , is 10 nm, and the scattered light is distributed uniformly to any direction.

3. Estimation of Stray Light Distribution

In the above section, the scattering light on the mirror is uniform in all direction, but actual scattering light intensity depends on a scattering angle (angle between the mirror's normal and scattering beam). There may be some scattering sources. It is attempted to find the source of the stray light and estimate its intensity distribution.

The stray light is often generated due to the reflection and/or scattering by the inside walls and optical components of the optical instrument. It is also thought that the stray light in the Imager is caused by the reflection and scattering on the inside walls and optical components. Regarding the reflection on the inside walls, it can be understood that they are painted black in the same way as a telescope for popular use, and the baffle and stop of the telescope remove the stray light from the walls due to telescope design. Therefore, a candidate for the source of the stray light should be components in the optical path: scan mirror, telescope (including three support boards of the secondary mirror, called a spider), and relay optics.

In general, the diameter of particles in the pigment of black paint is less than 0.1 micrometers. The painted surface is considered as a perfect diffuse reflection, and the reflectance of the black paint is less than 5 percent. On the other hand, the mirror surface accuracy (the standard deviation of surface roughness) of the telescope for popular use is several tens of nanometers, and the surface reflects light over 90 percent. Furthermore, scattering light from the mirror is concentrated within a small angle range. Therefore, the scattering light from the

spider is neglected in this discussion since it is smaller by one digit than the light from the mirror, even if it is illuminated by the sunlight concentrated by the primary mirror.

Although the mirror surface is very smooth, there is some micro roughness, and some particles exist due to absorption. Thus, imagine the situation wherein opaque disks that have a uniform diameter are irregularly distributed as a combination of the surface micro roughness and absorption particles. Since this situation can be replaced with another wherein circle openings that have the same size are irregularly distributed on an opaque board, it can be thought that the intensity of the diffraction light generated by N openings is N times compared with the intensity generated by one opening. And then the intensity of diffraction must show the distribution that is inversely proportional to the square of an angle from the mirror (or opaque board) normal.

Furthermore, the intensity of the sunlight that illuminates inside the Imager changes in the Imager case. If the sun is apart from the nadir direction, the sunlight that comes inside the Imager is reduced, and then the stray light is inevitably reduced. Part of the sunlight illuminating the scan mirror reaches the primary mirror, concentrates, and illuminates the scan mirror again. Although the detailed size of the telescope is unknown, as a result of rough ray trace, the relative sunlight intensity, S(α, β), is approximated by the following equations:

$$\alpha = \sqrt{(\mathbf{AZsun})^2 + (\mathbf{ELsun})^2} \qquad (5)$$

$$\beta = \sqrt{(AZsun - AZscan)^2 + (ELsun - ELscan)^2} \qquad (6)$$

$$S(\alpha,\beta) = p\left[1 - \frac{\beta}{23}\right] \cdot \left(-0.000432\alpha^2 - 0.014\alpha + 1\right) \qquad (7)$$

$$p[\mathbf{x}] \equiv \begin{cases} \mathbf{x}, & \mathbf{x} > 0 \\ \\ 0 & \mathbf{x} \leq 0 \end{cases} \qquad (8)$$

where AZ and EL are azimuth (east positive) and elevation (north positive) respectively in the coordinates that have the origin at nadir. They are indicated in degrees. The subscripts "sun" and "scan" mean the direction to the sun and line of sight respectively. β of Equation (6) is interpreted "SUN-LOS Angle." The left part of the right side of Equation (7), p[1-β/23], shows the ratio of the light that reaches the primary mirror to the light that passes Imager's aperture. Using these equations, the intensity of the diffraction light, D, is expressed as

$$\mathbf{D} = \mathbf{C} \cdot \mathbf{S}(\alpha,\beta) \cdot \beta^{-2} + \mathbf{Y} \qquad (9)$$

where C is a constant native to an imager, and Y is the term of diffraction pattern due to the secondary mirror and its spider. Equation (7) should be fully established for operational use because the output of Equation (7) is symmetric both in the east-west and north-south directions on α, but actually the scan mirror is elliptic and tilts 45 degrees to the direction of the earth, and then these produce an asymmetrical function. The reason the term of the light reaches the primary mirror that is introduced in Equation (7) is that the micro roughness of the primary mirror that is a curved surface mirror must be greater than the micro roughness of the scan mirror that is a flat mirror. For instance, if the micro roughness is twice as great, the scattering light is four times as great, as is clear from Equation (1). Therefore, it must be good that only the scattering by the primary mirror is considered approximately.

The diffraction by the secondary mirror and its spider should be notable, although their scattering light is ignored. Figure 4 shows the allocation of the spider in the left figure, and the diffraction pattern by the spider in the right figure. The diffraction pattern is the same as one when a bright star is observed using a telescope that has a spider. The distance between the bright and dark regions on the diffraction pattern is proportional to the thickness of the spider (support board). If the thickness is known, the diffraction pattern can be calculated. The diffraction pattern that is generated by the cover of the secondary mirror and shows a concentric circle can also be calculated. These diffraction patterns are indicated as term Y in Equation (9), which can be approximated as the same function as Equation (7), but it will be calculated by numerical analysis based on the ray trace for operational use.
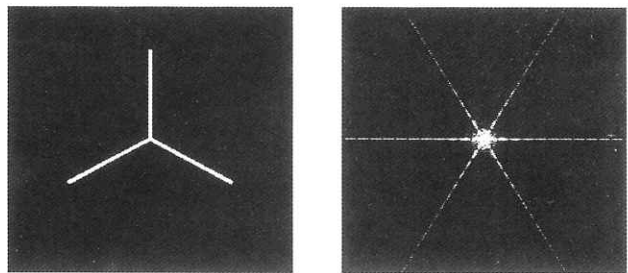

Figure 4. Diffraction Pattern by Spider

The left figure is the allocation of the spider that supports the secondary mirror. Interpreting the top of this figure as the north, the figure indicates GOES-10 Imager's orientation. There is no change in the pattern shown in the right figure even if the spider is upside down. The distance between bright and dark areas is proportional to the thickness of the spider.

4. Study using GOES Data

A study of the stray light using the GOES Imager data was conducted to verify that Equation (9) could express the stray light observed on the Imager. The imagery data of the GOES Imager was obtained from the GOES Project home page (http://rsd.gsfc.nasa.gov/goes/) of NASA/Goddard Space Flight Center (GSFC). The downloaded imagery data is based on the GOES Variable data received at GSFC. Data having 256 brightness levels is used for this study. All the data and information used in this study is in the public domain.

Figure 5 shows a catalog of the GOES Imager imagery data used for the study. The vertical and horizontal axes of the figure mean the date in 2002 and the time in UTC respectively. A dot in the figure indicates that imagery was used for the study. Local midnight time of GOES-8 and GOES-10 is 05 and 09 UTC respectively.

4.1 Distribution of Stray Light

An example of the stray light on GOES Imagers is shown in Figure 6. To watch the stray light easily, low light is enhanced in the visible channel, and the low-temperature region is also enhanced in Channel 2 (3.9 micrometers) by allocating low temperature to black and high temperature to white. Therefore, a part of the earth is saturated with the highest brightness level in Channel 2. The imagery of Channel 2 is enlarged twice to make it easy to view the space regions. The numeral indicated under the imagery shows the date and time of the imagery, and its format is YYMMDDhhmm (YY is the last two digits of the year, and MM, DD, hh, and mm are respectively month, day, hour, and minute in UTC).

It comes as a surprise to learn that very bright stray light is observed in the visible channel, although the GOES Imagers never scan the area within 6 degrees from the sun, in order to keep their safety.

The stray light is shown in Figures 7 and 8 on the relative position to the sun to show the features of the stray light more clearly. In these figures, the sun is located at the origin, the azimuth (east positive) is defined in the horizontal axis, and the elevation (north positive) is defined in the vertical axis. Observations before midnight are positioned at the right side against the origin, and observations in the summer are positioned below the origin. Three concentric circles show the distance from the sun. In these figures, low light in the visible channel and low temperature in Channel 2 are enhanced in the same way as in Figure 6, but a crescent earth in the visible channel and the earth in Channel 2 are not used. When more than one observation data exist at a point, the highest intensity is employed. Since the only space regions provide information on the stray light, some of the map of the stray light has no data in Channel 2.

From these figures, it is confirmed that the stray light is in a radial pattern on GOES-8 visible, Channel 2, and GOES-10 Channel 2. The allocation of the radial stray light meets the diffraction pattern of the spider shown in Figure 4. On the other hand, no linear pattern is observed, and bright arc-shaped patterns are observed on GOES-10 visible. The diffraction pattern of the spider cannot be observed when an astronomical telescope that observes a fixed star is out of focus. Since an out-of-focus situation affects the visible channel, rather than

the shortwave infrared, this phenomenon may be caused by the lack of focus.

4.2 Linear Stray Light

Two pieces of evidence exist to show that the linear stray light is the diffraction pattern caused by the spider. First, a cross section of the linear stray light is shown in Figure 9, and radiances along lines (A-B, C-D, and E-F) in the imagery are shown at the lower part of the image. From this figure, it can be read that the cross section of the linear stray light has good symmetry with respect to the ridge of the linear stray light. The linear stray light of the left figures is a part of a circle, and light in a figure at the upper right is a radial, linear stray light from the sun. It can be noticed that the radial, linear stray light has a width of 0.5 degrees, that is, an apparent diameter of the sun. Furthermore, measuring the radiance along the ridge of the linear stray light, it is inversely proportional to the square of an angle from the sun shown in the lower right. This also shows that the linear stray light is caused by the diffraction pattern of the spider.

Another important piece of evidence is observed on July 28, 2002, at 0930 by GOES-10. The sunlight reflected on the water surface can be observed in the top of Figure 10, visible imagery. Enhancing this imagery, circular light (areas indicated by arrows) comes up shown in the second imagery from the top. Viewing the same area in Channel 2 (the third imager from the top), three lines of light are observed. These lines have intervals of just 60 degrees. There is no doubt that these light lines are the diffraction pattern of the spider. Moreover, some bright-and-dark cycles of about 5 pixels are observed

at the linear light of O-A and O-B. If this is the same bright-and-dark as shown in Figure 4, it is estimated that the thickness of the spider of the GOES-10 Imager is 7 mm, which meets the actual thickness that is read from a drawing in the public domain (i.e., GOES I-M Data Book at http://rsd.gsfc.nasa.gov/goes/). Three lines of light viewed in Figure 10 are rotated about 7 degrees counterclockwise, as compared with Figure 4. It is thought that the rotation is caused by the Image Motion Compensation (IMC) function or the focal plane rotation.

Paying attention to the visible imagery here again, the line of light is not observed in the visible channel. This means that something (probably ice or cracks on lenses, contamination on mirror surfaces, etc.) works to counteract the diffraction pattern of the spider.

4.3 Verification of Stray Light Estimation

Equation (9) is a function of α and β. Once measuring the stray light of constant β, that is, the area where there is a fixed position relative to the sun, the contribution of α must become clear.

Figure 11 shows the intensity of the stray light with the traces of the small area that is fixed relative to the position of the sun using the observation data of GOES-8 0545 UTC. The locations of stray light measurement are shown in the bottom figure, and the upper left figure shows the intensity of the stray light in the vertical axis and the date in the horizontal axis. The relative intensity of the stray light as compared with the highest intensity of each trace is shown in the upper right. Since the horizontal axis of the figure is allocated to α, it shows decreases in intensity with increases in

α. Since S decreases 15 percent with a change in α from 19 to 21.5 degrees on the condition that β is constant based on Equation (7), the validity of Equation (7) is roughly confirmed by the measurement shown here, although the data vary widely.

Trace No.5 measures the arc-shaped pattern of the stray light with its center at the sun, and its intensity shows a different behavior as compared with Equation (7). It is thought that the behavior is caused by a change in solar illumination on the secondary mirror, since the arc-shaped pattern is the diffraction one generated by the cover of the secondary mirror that is smaller than the primary mirror; thus the change is greater than a change on the primary mirror. Figure 12 verifies this understanding. It also shows the results of stray light measurement at a fixed relative position against the sun in the same way as Figure 11, but for GOES-10. It is shown in the upper figure that the intensity of the linear stray light can be expressed as a function of α. A change in the relative intensity of the stray light is greater than that calculated by Equation (7), because the spider is smaller than the primary mirror; thus a daily change in solar illumination on the spider is remarkable. The results of simple ray trace are shown at the right of Figure 12, which agrees with the observed change.
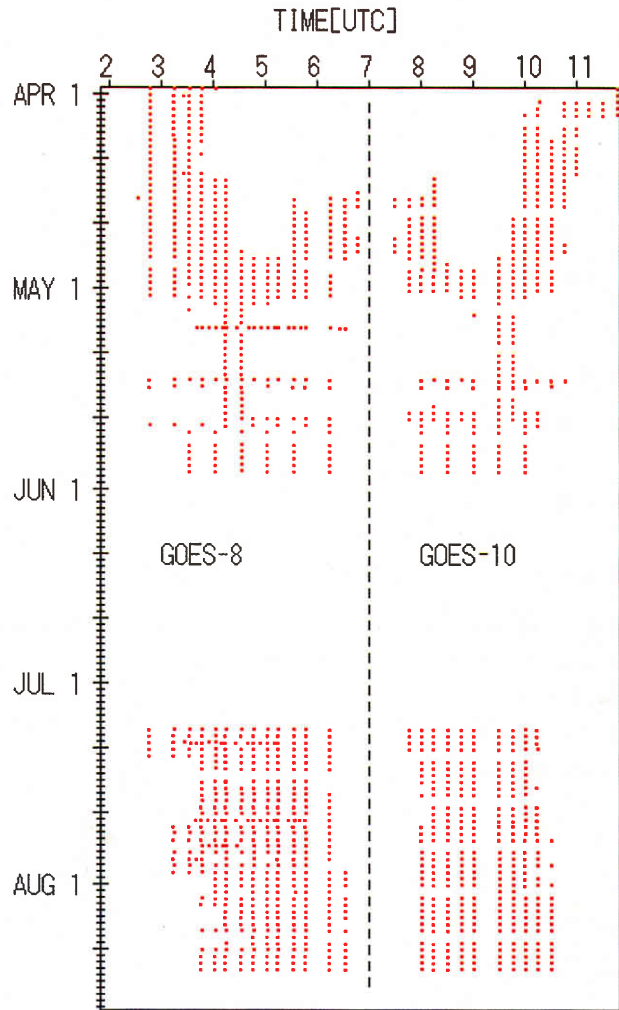

Figure 5. Catalog of GOES Data used for Stray Light Study

This shows a catalog of the GOES Imager imagery data used for the study. The vertical and horizontal axes of the figure mean the date of 2002 and time in UTC respectively. A dot in the figure indicates that the imagery was used for the study. Local midnight time of GOES-8 and GOES-10 is 05 and 09 UTC respectively.

GOES-8
Visible

GOES-8
Channel 2
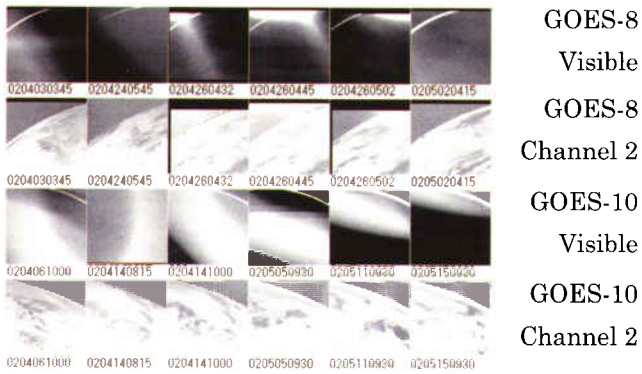
GOES-10
Visible

GOES-10
Channel 2

Figure 6. Example of Stray Light on GOES Imagers

Low light is enhanced in the visible channel, and low-temperature regions are also enhanced in Channel 2 (3.9 micrometers) by allocating low temperature to black and high temperature to white. The imagery of Channel 2 is enlarged twice to make it easy to view the space regions. The numeral indicated under the imagery shows the date and time of the imagery, and its format is YYMMDDhhmm (YY is the last two digits of year, and MM, DD, hh, and mm are respectively month, day, hour, and minute in UTC.)

visible spectrum and low temperature in Channel 2 are enhanced in the same way as in Figure 6. Bright white indicates strong stray light.
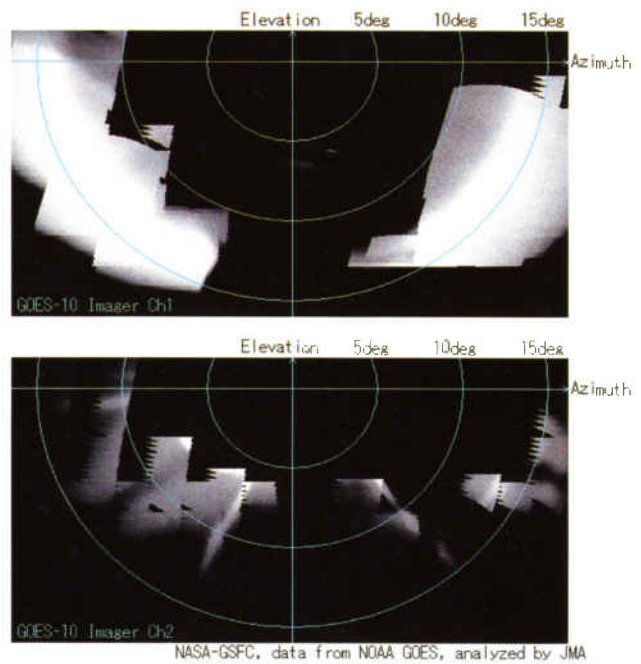

Figure 8. GOES-10 Stray Light Map

This figure shows the distribution of GOES-10 stray light. The definition of the figure is the same as in Figure 7. The reason why a visible arc breaks at the center of the figure is the effect of the space look of the Imager, but the reason why the arc is not symmetrical is unknown. The linear stray light in the bottom figure is curved since a satellite longitudinal position changed.

Figure 7. GOES-8 Stray Light Map

The distribution of the stray light on the relative position against the sun is shown. The top is the visible channel, and the bottom is Channel 2. Azimuth (east positive) is defined in the horizontal axis, and the elevation (north positive) is defined in the vertical axis. The sun is located at the origin, and low light in the

GOES-8 02-07-23 0545   GOES-8 02-04-18 0615   GOES-10 02-05-06 0930
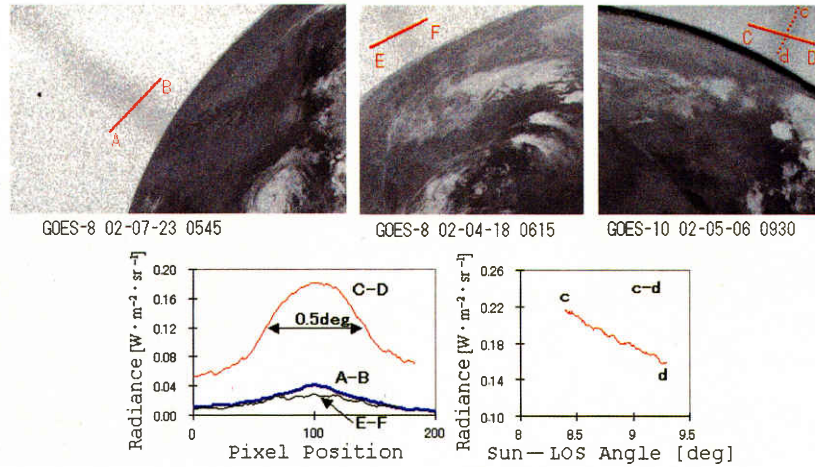
Figure 9. Cross Section of Linear Stray Light

This figure shows a cross section of the linear stray light. Three cases are shown here, and radiance at a bar in the imagery is shown below. It can be read that the cross section of the linear stray light has good symmetry with respect to the ridge of the linear stray light. The linear stray light of the left figures is a part of a circle, and one in a figure at the upper right is a radial, linear stray light from the sun. It can be noticed that the radial, linear stray light has a width of 0.5 degrees, that is, an apparent diameter of the sun. Furthermore, measuring the radiance of the ridge of the linear stray light shown in the lower right, it is inversely proportional to the square of an angle from the sun.

GOES-10 02-07-28 0930
Visible

GOES-10 02-07-28 0930
Visible (Enhanced)
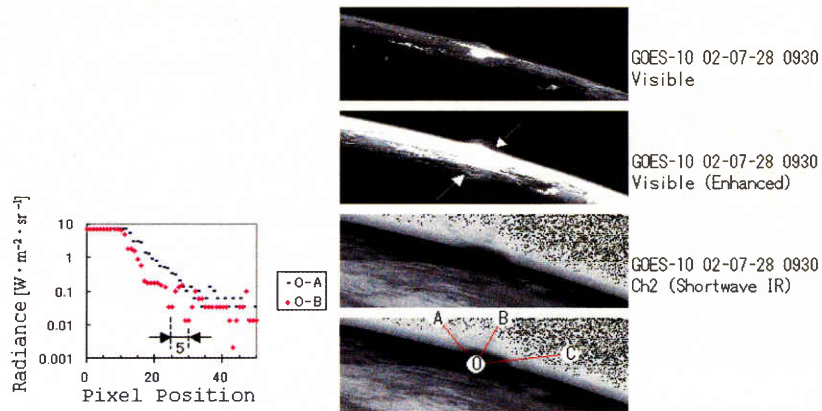
GOES-10 02-07-28 0930
Ch2 (Shortwave IR)

Figure 10. Sunlight Reflected on Water Surface

The sunlight reflected on the water surface shows interesting phenomena. The images shown here are the visible channel and Channel 2 observed by GOES-10 on July 28, 2002, at 0900. The top visible image shows the sunlight reflected on the water surface. Enhancing this imagery, circular light (areas indicated by arrows) comes up shown in the second imagery from the top. Viewing the same area in Channel 2 (the third image from the top), three lines of light are observed. These lines have intervals of exactly 60 degrees. The left figure shows the radiance on O-A and O-B. Some bright-and-dark cycles of about 5 pixels are observed.

A comparison between the observed and estimated stray light intensity is conducted to verify Equation (9), which estimates the intensity of the stray light. Figure 13 shows an area for measuring radiance in the space regions with a square frame. The area has 50 by 50 pixels on the image, and the average value of the radiance is calculated. The top and bottom figures indicate the GOES-8 and GOES-10 areas respectively. Figure 14 shows the radiance

of the areas measured by plotting an angle between the sun and imager's Line-Of-Sight (LOS) in horizontal axis and the space radiance, that is, the intensity of the stray light in the vertical axis. GOES-8 indicates the distribution that is inversely proportional to the sun-LOS angle, but GOES-10 has no clear relation with the sun-LOS angle, since the radial stray light is as shown in Figure 8.

A comparison between the observed and estimated intensity is conducted in the upper left of Figure 15, that is, the observed intensity plotted in the vertical axis and the estimated value, D, of the stray light when C=1[W m^{-2} sr^{-1}] in the horizontal axis. Assuming that the diffraction by the secondary mirror and its spider, Y, is zero to simplify the calculation, D is calculated in this figure. From the figure, the value of 25.4[W m^{-2} sr^{-1}] is obtained for C. The frequency distribution of the observed stray light intensity at intervals of 1 Kelvin is shown in the upper right, and it shows that the stray light exists over 7 Kelvin. The bottom chart shows the frequency distribution of the estimation error by Equation (9) when the value C of 25.4[W m^{-2} sr^{-1}] is used for the calculation at intervals of 0.2 Kelvin. It shows that 98 percent of cases exist in the range of -1 to +1 Kelvin, and then it is expected that the error will decrease, since the Y term in Equation (9) will be used for operational work.

Since the value C is obtained in Figure 15, the stray light intensity at a small value of the sun-LOS angle can be estimated. As shown in Table 1, the pixel value of the imagery of greater than 300 Kelvin is saturated at an observable maximum temperature when the sun-LOS angle is 2.0 degrees. Moreover 273 Kelvin is saturated

at 1.7 degrees; thus, effective cloud imagery cannot be obtained due to the saturation. In a practical manner, since GOES-8 does not scan the area within 6 degrees from the sun in order to guarantee the telescope's safety, the cloud imagery is not saturated at the observable maximum temperature, but there is a possibility that this saturation phenomenon will be observed on MTSAT-2 and future GOESs, since they will scan more closely to the sun. The saturation cannot be corrected, since information on the cloud imagery is lost on saturated pixels at the maximum temperature.

Saturation Temperature [K]	Sun-LOS Angle [deg]
300	2.0
273	1.7

Table 1. Relation between GOES-8 Saturation Temperature and Sun-LOS Angle

Assuming that the observable maximum temperature of the Imager is 330 Kelvin when no stray light exists, the saturation temperature is defined by the observable maximum temperature that is reduced by the stray light. 273 Kelvin and up cannot be observed at the sun-LOS angle of 1.7 degrees.

There is one difficulty of the verification of stray light estimation on GOES-10 that is observed with prominent linear stray light. Because no orbital information on a satellite in the GOES data is used for this study, an accurate position against the sun could not be estimated. Since the intensity changes 50 percent if the position of the linear stray light moves 0.25 degree, a reliable estimation of the accuracy cannot be obtained without accurate information on the satellite position. Thus the result of the correction of the linear stray light in the case that the sun position can be calculated accurately is presented here.

Figure 16 shows the correction of the linear

stray light using the full disk imagery of GOES-10 on August 7, 2002, at 0900 UTC. The view on the right is the original imagery before the correction, and its low-temperature region is enhanced to make it easy to view the stray light. The linear stray light disappears in the corrected imagery shown in the left figure. The frequency distribution charts of the brightness temperature at the space regions are shown under the imagery, which show the estimation error is less than 1 Kelvin since the brightness temperature of the space indicates the remaining intensity of the stray light. The following equations are used to correct the linear stray light.

$$\begin{pmatrix} Tx \\ Ty \end{pmatrix} = \begin{pmatrix} \cos\theta & -\sin\theta \\ \sin\theta & \cos\theta \end{pmatrix} \begin{pmatrix} AZscan - AZsun \\ ELscan - ELsun \end{pmatrix}$$

$$Y = \frac{Y_0}{Ty^2} \exp\left[-\frac{Tx^2}{2w^2}\right]$$

(10)

where Tx and Ty are the x and y components of rotated coordinates to fit the linear stray light on its y-axis. θ is a rotation angle of the linear stray light, and the value of θ is -30°, 30°, or 90°. Y_0 and w are the coefficients that determine the shape of the linear stray light, and their values are approximately 14.5° and 0.28° respectively.

The difference in stray light distribution between GOES-8 and GOES-10 can be understood as a difference of the light source. It is thought that the stray light from a mirror is prominent on GOES-8 because its distribution decreases quickly with increases in the angle from the sun, while the stray light from the secondary mirror and spider is prominent on GOES-10 since its distribution shows no clear relation with the angle from the sun. As GOES-10 was launched 3 years after GOES-8, it is natural to think

that technical improvement during 3 years and lessons learned on GOES-8 have a good effect on GOES-10. Improvement on manufacturing technology and the cleanliness level of the mirrors reduce the stray light from the mirror, and reduce the degree of the telescope's being out of focus; thus the stray light from the secondary mirror and spider is prominent as a result of them. Since the MTSAT-2 Imager is an extension of GOES imagers, the stray light that is similar to GOES-10 will be observed.
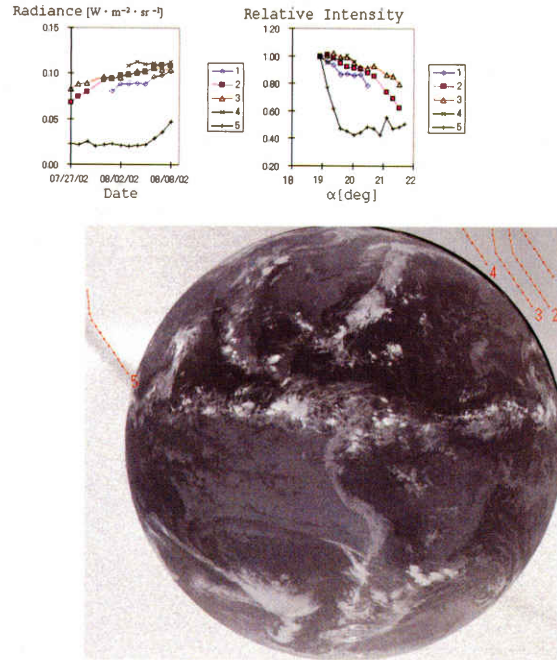

Figure 11. Trace of Stray Light Intensity on Sun-synchronized Space Regions on GOES-8

The intensity of the stray light is shown here, which is measured with the traces of the small area that is a fixed relative position to the sun using the observation data of GOES-8 0545 UTC. The areas of stray light measurement are shown in the bottom figure, and the upper left figure shows the intensity of the stray light in the vertical axis and the date in the horizontal axis.
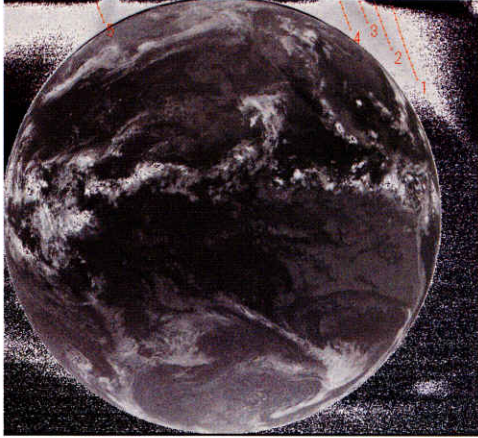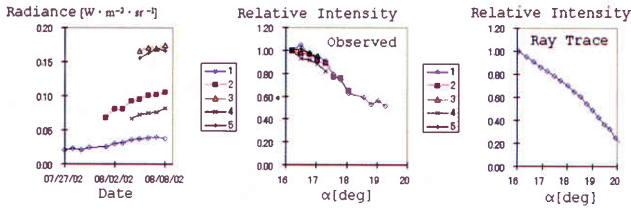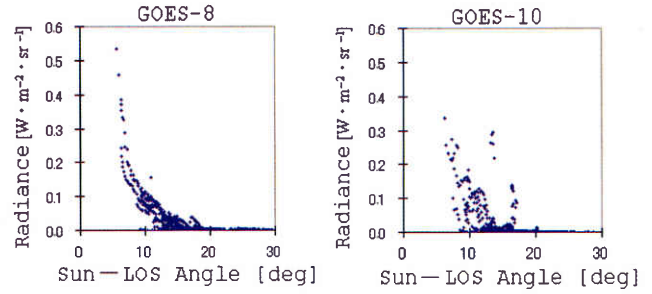
Figure 14. Space Radiance

Figures plot an angle between the sun and imager's Line-Of-Sight (LOS) in horizontal axis and the space radiance, which is the intensity of the stray light in the vertical axis. GOES-8 indicates a distribution that is inversely proportional to the sun-LOS angle, but GOES-10 has no clear relation with the sun-LOS angle because of the radial stray light, as shown in Figure 8.

Figure 12. Trace of Stray Light Intensity on Sun-synchronized Space Regions on GOES-10

The definition of the figure is the same as Figure 11, but the image time is 0900 UTC on GOES-10. The upper right shows the relative sunlight intensity that illuminates the spider.
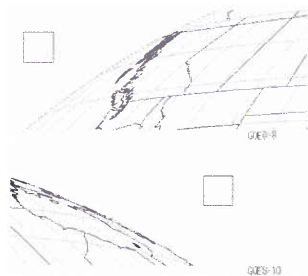
Figure 13. Area for Measuring Space Radiance

The average value of the radiance in square frames is calculated. The top figure shows an area for GOES-8, and the bottom is GOES-10. The area has 50 by 50 pixels on the imagery.
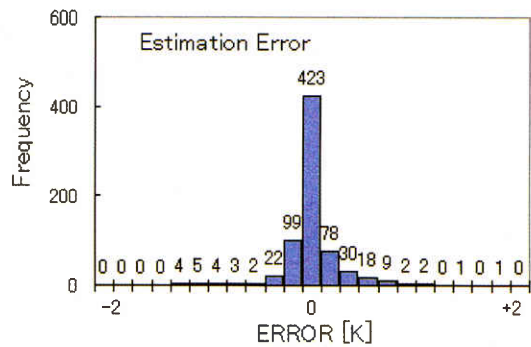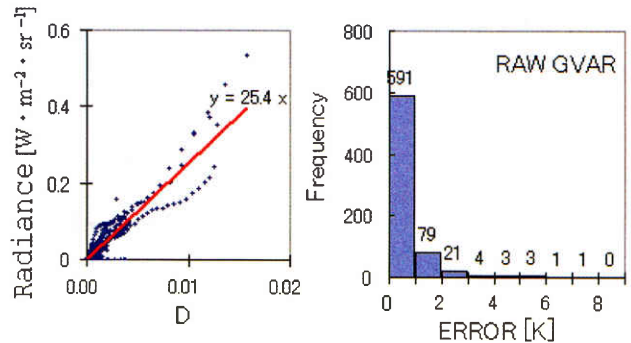
Figure 15. Estimation Error of Stray Light on GOES-8

The upper left is the plotted observed intensity in the vertical axis and the estimated value, D, of the stray light when $C=1[W\ m^{-2}\ sr^{-1}]$ in the horizontal axis. Assuming that the diffraction by the secondary mirror and its spider, Y, is zero to simplify calculation, D is calculated in this figure. From the figure, the value C of $25.4[W\ m^{-2}\ sr^{-1}]$ is obtained. The frequency distribution of the observed stray light intensity at intervals of 1 Kelvin is shown in the upper right, and it shows that the stray light exists over 7 Kelvin. The bottom chart

shows the frequency distribution of the estimation error by Equation (9) when the value of 25.4[W m^{-2} sr^{-1}] is used for C in the calculation at intervals of 0.2-Kelvin. It shows that 98 percent of cases exist in the range of -1 to +1 Kelvin, and then it is expected that the error will decrease, since the Y term in Equation (9) will be used for operational use.
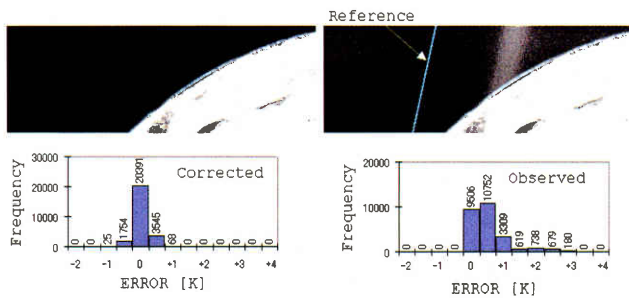

Figure 16. Example of Correction for Linear Stray Light on GOES-10

This shows the correction of the linear stray light using the full disk imagery of GOES-10 on August 7, 2002, at 0900 UTC. The right view is the original imagery before the correction, and its low-temperature region is enhanced to make it easy to view the stray light. The linear stray light disappears in the corrected imagery shown in the left figure. The charts of the frequency distribution are shown under the imagery. The stray light generated by a mirror is also corrected based on the reference area of the original imagery with C=12.2[W m^{-2} sr^{-1}].

5. Measurement and Correction of Stray Light

The stray light of the imager should be measured when the imager is manufactured and tested on the ground; however, it may not be easy to use an artificial sunlight source to measure it. On-orbit measurement during post-launch checkout is required at the least.

Before Imager mission operation, the intensity of the stray light is measured by repeatedly scanning the space region in the west (or east) of the earth shown in Figure 17. After one imaging of this region, the sun would move to the east just a distance equal to the width of the region; thus the space radiance is observed

without a gap by using repeated imaging. The size of the region is 1.6 (east-west) by 17.6 (north-south) degrees. It is desired that the stray light observation using this technique will be planned about every two weeks to obtain at least three measurements everywhere. During the Imager mission operation, this kind of observation cannot be operated, so that the data of the space regions acquired in full disk or northern hemisphere observations will be used. Based on these measurements and information, coefficients of the stray light estimator that is an expansion of Equation (9) are determined, and then they are used to correct and monitor the stray light.

The stray light is predicted ahead of time, and corrected based on the predicted value for MTSAT-2 operation. Since the effect of the stray light is limited around midnight, even if massive calculations such as a ray trace will be required, it is sufficient to do the calculations in the daytime.
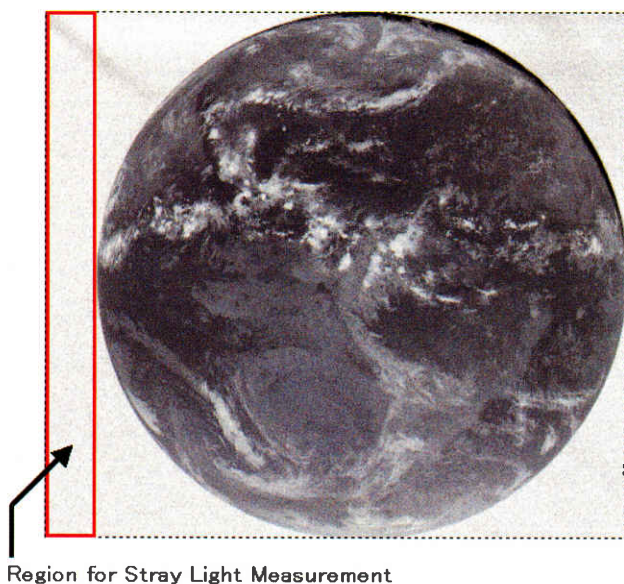
Region for Stray Light Measurement

Figure 17. Measurement Area of Stray Light

This figure shows an area for measuring the intensity of the stray light. Before Imager mission operation, the intensity of the stray light is measured by scanning the space region in the west (or east) of the earth. The size of the region is 1.6 by 17.6 degrees.

6. Application to Sounder

It is known that a prominent striped pattern appears on sounder imagery around midnight in and near eclipse seasons on the GOES Sounder. The Cooperative Institute for Meteorological Satellite Studies (CIMSS) demonstrates GOES sounder imagery, and it shows that the striped pattern is especially remarkable in May and August. One example of the striped pattern is shown in Figure 18, which is obtained from http://cimss.ssec.wisc.edu/goes/realtime/. The striped pattern is observed from channels 13 to 18, and it is thought that the pattern is caused by differences of the detector output of the sounder, not by considering the features of an atmospheric phenomenon. It is attempted here to explain the striped pattern by the stray light.

Since the scanning of the sounder is different from the Imager and the sounder does not scan the space widely, the direct measurement of the stray light is limited to the space look that is obtained during sounding and blackbody observation. However, no zero correction of sounder output is operated, so that the absolute value of the detector output can be known. Since an angular distance between detectors on the sounders is greater than the imager's one, it may be that there is a difference of the stray light intensity that reaches the detectors, and the difference is visualized as a striped pattern.

The value that is explored here is a difference of the stray light between the sounding (observation of earth region) and the space look. Assuming the angular distance between the sounding and space look regions is 15 degrees, the difference of the stray light caused by intervals of 1 hour must be observed as compared with two space look data at intervals of 1 hour, because the sun moves 15 degrees during an hour. If it is observed that the difference of the stray light is uneven among the detectors, it must appear as a striped pattern on the sounder imagery. A point to note here is that the space look data of the sounder contains radiance from the scan mirror, telescope and so on, so that the effect of their temperature changes should be considered. The effect is calculated by data from the blackbody observation. The concept of the technique is shown in Figure 19, and the equations are as follows:

$$\left. \begin{array}{l} \Delta R_n = R_{n,sp,T1} - R_{n,sp,T2} - \left(r_{n,bb,T1} - r_{n,bb,T2}\right) + \left(R_{n,bb,T1} - R_{n,bb,T2}\right) \\[2mm] \overline{\Delta R} = \dfrac{\Delta R_1 + \Delta R_2 + \Delta R_3 + \Delta R_4}{4} \\[2mm] \sigma = \sqrt{\dfrac{1}{4}\left[\displaystyle\sum_{n=1}^{4}\left(\Delta R_n - \overline{\Delta R}\right)^2\right]} \end{array} \right\} \quad (11)$$

where R and r are the radiance calculated by observed counts and blackbody temperature respectively. The subscripts: n, sp, bb, T1, and T2 mean detector number, space look, blackbody look, time in interest, and time in reference, respectively.

Figure 20 shows the stray light unevenness of the GOES-8 Sounder calculated by Equation (11). The figure plots unevenness in the vertical axis and the date in the horizontal axis. It shows that the unevenness increases in May and August, and agrees with the observation. If the stray light causes the striped pattern, it will be possible to remove the striped pattern by applying the technique of the stray light estimation. The data used for this calculation was provided by the National Oceanic and Atmospheric Administration (NOAA), which is the same information as the data distributed by GVAR into the public domain.
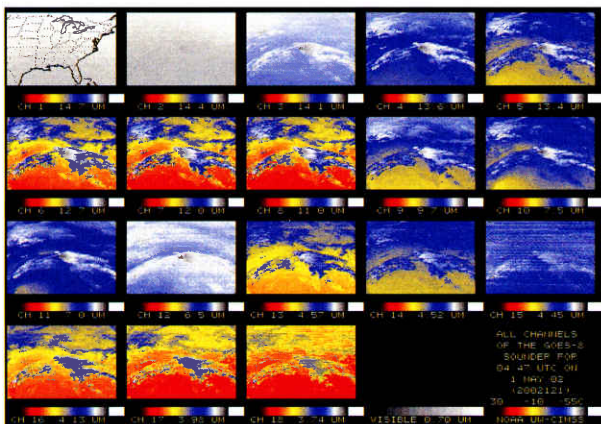

Figure 18. Example of Striped Pattern on GOES Sounder Imagery

This imagery was obtained from http://cimss.ssec.wisc.edu/goes/realtime/. The striped pattern is observed from channels 13 to 18.
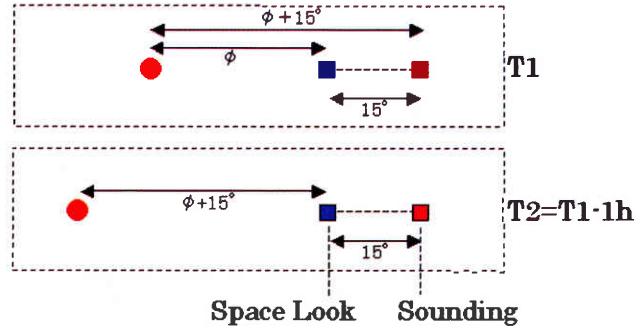

Figure 19. Concept of Technique to Estimate Stray Light Unevenness

Assuming the angular distance between the sounding and space look regions is 15 degrees, the difference of the stray light caused by this angular distance is approximated by comparison with the space look data at intervals of 15 degrees.
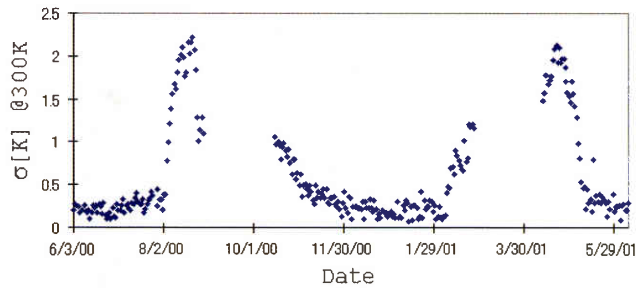

Figure 20. Stray Light Unevenness on GOES-8 Sounder

This shows the stray light unevenness of the GOES-8 Sounder calculated by Equation (11). The figure plots unevenness in the vertical axis and the date in the horizontal axis. It shows that the unevenness increases in May and August. Two observation slots: 0446 and 0545 were used. The data used for this calculation was provided by the National Oceanic and Atmospheric Administration (NOAA), which is the same information as the data distributed by GVAR into the public domain.

7. Conclusion

Equations for correction based on the physical discussions were developed to correct the stray light on the Imager in this study, and they were verified using GOES data. However, more terms should be added, and improved equations should be used to verify its accuracy. Since considerable high-resolution GOES image data, including orbital information, will be required to verify the accuracy, it is desired to establish collaboration on this study with NOAA, which operates the GOES satellites.

The technique of predicting and correcting the stray light of the Imager was developed. The development of the technique is summarized as follows.

- Based on physical discussions, equations were developed to estimate the stray light caused mainly by the primary mirror and spider.
- Linear stray light is observed on GOES imagers.
- The stray light caused by a mirror is prominent on GOES-8, while light caused by the spider is prominent on GOES-10.
- The verification of the equations was conducted using GOES data, and it showed that an estimation error of 1 Kelvin or less would be achieved.
- Orbital information is required, since an accurate estimation of the linear stray light is needed for improvement of the estimation.
- A technique to measure the stray light efficiently in orbit was developed.
- The correction of the stray light is based on its prediction, and the prediction can be calculated in the daytime, although the calculations are massive.
- The stray light may be one of the causes of the striped pattern observed on GOES sounder imagery, and the striped pattern will be correctable.

Since the shortwave infrared channel is especially effective in the detection of nighttime fog and low-level clouds, it is required to remove the stray light to keep the effectiveness of the shortwave infrared channel. The technique for the stray light correction developed here will be in operation for MTSAT-2 with fully established equations for the estimation and the verification of their prediction accuracy.

All the GOES data used in this development is in the public domain.

Reference

M. Born and E. Wolf, 1975: Principles of Optics, Pergamon Press, Oxford, UK

イメージャの迷光補正について

木川誠一郎

概　要

　運輸多目的衛星新2号のイメージャは波長3.75マイクロメートルのチャンネルを有し、夜間の霧や下層雲の検出に効果を発揮すると期待されている。この波長帯では真夜中付近にイメージャの迷光が観測されることが、GOES（Geostationary Operational Environmental Satellite）イメージャの観測データから明らかになっている。そこで、迷光を予測し、補正する手法が開発された。予測は物理的考察に基づく推定式により行い、その予測に基づいて観測データを補正する。GOESデータを用いて推定式の検証が行われ、推定誤差1K以内を実現できることが明らかになった。また、迷光の推定技術を用いれば、GOESサウンダに見られる縞模様の除去もできそうである。ここでは、運輸多目的衛星新2号において運用される予定の迷光補正について、概要を報告する。